

# Online wave estimation using vessel motion measurements<sup>\*</sup>

Astrid H. Brodtkorb<sup>\*</sup> Ulrik D. Nielsen<sup>\*,\*\*</sup>  
Asgeir J. Sørensen<sup>\*</sup>

<sup>\*</sup> Centre for Autonomous Marine Operations (NTNU AMOS),  
Department of Marine Technology, Norwegian University of Science  
and Technology (NTNU), Otto Nielsens vei 10, 7491 Trondheim,  
Norway (e-mails: [astrid.h.brodtkorb@ntnu.no](mailto:astrid.h.brodtkorb@ntnu.no),  
[asgeir.sorensen@ntnu.no](mailto:asgeir.sorensen@ntnu.no))

<sup>\*\*</sup> DTU Mechanical Engineering, Technical University of Denmark,  
DK-2800 Kgs. Lyngby, Denmark (e-mail: [udn@mek.dtu.dk](mailto:udn@mek.dtu.dk))

**Abstract:** In this paper, a computationally efficient *online* sea state estimation algorithm is proposed for estimation of the *onsite* sea state. The algorithm finds the wave spectrum estimate from motion measurements in heave, roll and pitch by iteratively solving a set of linear equations. The main vessel parameters and motion transfer functions are required as input. Apart from this the method is signal-based, with no assumptions on the wave spectrum shape, and as a result it is computationally efficient. The algorithm is implemented in a dynamic positioning (DP) control system, and tested through simulations in different sea states, with heading changes. Discrete stability analysis is performed to find iteration gains in the algorithm.

© 2018, IFAC (International Federation of Automatic Control) Hosting by Elsevier Ltd. All rights reserved.

*Keywords:* sea state estimation, dynamic positioning

## 1. INTRODUCTION

Complex marine operations are moving further from shore, into deeper waters, and harsher environments. The operating hours of a vessel are weather dependent, and good knowledge of the prevailing weather conditions may ensure cost-efficient and safe operations, especially considering operations with high levels of autonomy (Ludvigsen and Sørensen, 2016), and having a fast and reliable method for obtaining an estimate of the *onsite* sea state is useful both directly in control systems for adaption purposes, and in decision support systems to aid the decision making process, with or without the operator onboard the vessel.

Estimating the sea state based on ship motion measurements has had considerable attention during the last 10-12 years (Tannuri et al., 2003; Simos et al., 2007; Pascoal and Guedes Soares, 2009; Iseki, 2010; Montazeri et al., 2016), see Nielsen (2017) for a summary. Recently, a new approach was proposed in Brodtkorb et al. (2018), where the point-wise wave spectrum was estimated by an iteration procedure based on motion measurements of a vessel in dynamic positioning (DP), without forward speed, in a long-crested sea state. The mean wave direction was found by considering the mean wave energy of the wave spectrum candidates. Nielsen et al. (2018) extended the method to include correction for forward speed and for short-crested sea states. Both approaches are *offline* in the sense that they run on data obtained from full-scale vessel motion data or simulations as a post-process.

<sup>\*</sup> This work was supported by the Research Council of Norway through the Centres of Excellence funding scheme, project number 223254 - NTNU AMOS.

The main contributions of this paper include the implementation of the spectral calculation method in Brodtkorb et al. (2018) with the direction estimation procedure from Nielsen et al. (2018) in a Matlab/Simulink dynamic positioning (DP) control system for *online* estimation of the sea state. The algorithm was tested in simulations of a research vessel conducting DP operations with heading changes. Sensitivity analysis for the estimation procedure, focusing on the gains in the iteration procedure, and the calculation of response spectra from measurement time series was done. Discrete stability analysis was used to find suitable values for the iteration gains.

The paper is organized as follows: Section 2 gives some background information related to vessel motion modeling and spectral theory. An overview of the sea state estimation algorithm is given in Section 3, and some implementation aspects are discussed in Section 5. In Section 6 the simulation setup, cases and results are given, before the results are discussed. Section 7 concludes the paper.

## 2. SPECTRAL THEORY BACKGROUND

For control design purposes, the vessel motion is usually modeled as a mass-damper-restoring system subject to the loads from current, wind, and waves (Fossen, 2011). For ships in DP the thrusters will produce mean and slowly varying generalized forces in the horizontal plane to cancel those from the environment. Therefore the DP control system influences the surge, sway and yaw motion of ships directly, and the *heave* ( $z$ ), *roll* ( $\phi$ ) and *pitch* ( $\theta$ ) motions are more suited for sea state estimation. The measurements of heave, roll and pitch are recorded

in the *body*-frame, which is defined with positive x-axis pointing towards the bow, positive y-axis pointing towards starboard, and with positive z-axis pointing down, see Figure 1. In DP the vessel has zero or low forward speed, so that the frequency of encounter is assumed to be the same as the incident wave frequency,  $\omega_e = \omega_0 = \omega$ .

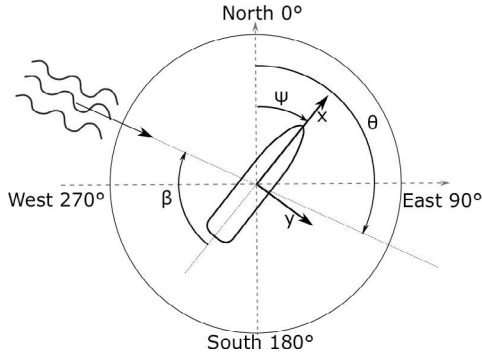


Fig. 1. Definition of the wave propagation direction  $\Theta \in [0, 360]^\circ$ , heading of the vessel  $\psi$ , and relative wave direction  $\beta$ . Starboard incident waves have  $\beta \in (-180, 0]^\circ$ , and port incident waves have  $\beta \in [0, 180]^\circ$ .

In this paper, it is assumed that the waves are long-crested, with propagation direction  $\Theta$ , as defined in Figure 1, and that there is a linear relationship between the wave amplitude and the response amplitude. The wave direction relative to the vessel heading is  $\beta$ , with  $\beta = 180^\circ$  being head sea, and  $\beta = 0^\circ$  being following sea.

The relationship between the wave amplitude and the vessel response amplitude (here only heave, roll and pitch are considered) is given by the complex-valued (motion) transfer functions  $X_i(\omega, \beta)$ , which can be calculated using hydrodynamic software codes<sup>1</sup>. The complex-valued cross-spectra  $R_{ij}(\omega)$  can be calculated as:

$$R_{ij}(\omega) = X_i(\omega, \beta) \overline{X_j(\omega, \beta)} S(\omega), \quad (1)$$

where  $R_{ij}(\omega)$ ,  $i, j = \{z, \phi, \theta\}$  are the heave, roll, and pitch response spectra,  $\overline{X_j(\omega, \beta)}$  is the complex conjugate of the transfer functions in heave, roll and pitch for the relative wave direction  $\beta$ , and  $S(\omega)$  is the wave spectrum. When  $i \neq j$ ,  $R_{ij}(\omega)$  is complex-valued, and when  $i = j$  the imaginary part is zero,  $\mathcal{I}m(R_{ii}(\omega)) = 0$ . The imaginary parts of the cross spectra pairs have opposite signs, i.e.,  $\mathcal{I}m(R_{ij}(\omega)) < 0 \Leftrightarrow \mathcal{I}m(R_{ji}(\omega)) > 0$ , that are dependent on the incident wave direction. This is used later to distinguish whether the waves are starboard or port incident. The cross-spectra are calculated using a Matlab/Simulink block based on Welch cross-spectral estimation method (Welch, 1967).

For numerical stability of the estimation procedure, we consider the magnitudes of (1),

$$|R_{ij}(\omega)| = |X_i(\omega, \beta) \overline{X_j(\omega, \beta)}| S(\omega), \quad i, j = \{z, \phi, \theta\} \quad (2)$$

where

$$|R_{ij}(\omega)| = \sqrt{[\mathcal{R}e(R_{ij}(\omega))]^2 + [\mathcal{I}m(R_{ij}(\omega))]^2}. \quad (3)$$

We assume that

<sup>1</sup> Here ShipX (Sintef Ocean, 2017) is used, but WAMIT (WAMIT Inc., 2017) is also widely used.

- (A1) The response spectra  $R_{ij}(\omega)$  are computed based on *stationary* measured responses in heave, roll and pitch.
- (A2) The motion transfer functions  $X_i(\omega, \beta)$ ,  $i = \{z, \phi, \theta\}$  are known.
- (A3) The wave spectrum is stationary over the time span we are examining, i.e.,

$$S^+(\omega) = S(\omega), \quad (4)$$

where “+” denotes the *next discrete time step*.

### 3. SEA STATE ESTIMATION ALGORITHM

The sea state estimate, consisting of a point-wise wave spectrum estimate and a wave direction estimate, is computed in two main steps, as illustrated by Figure 2. They are described in detail subsequently, but summarized as follows: Firstly, the response spectrum magnitudes in heave, roll and pitch,  $|R_{ij}(\omega)|$ , and the motion transfer functions of the ship are used to find an initial estimate of the unknown wave spectrum  $S(\omega)$ . This is done by solving (1) through iteration, and results in a matrix of wave spectrum candidates. Secondly, the energy in the

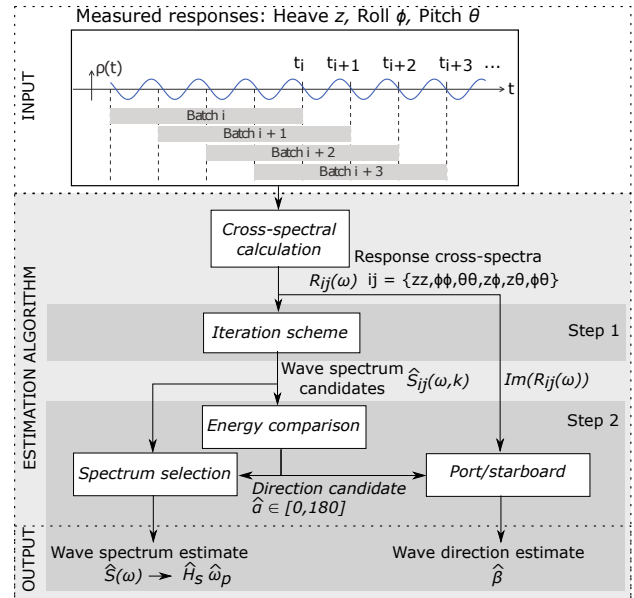


Fig. 2. Illustration of the proposed sea state estimation method, in two main steps. Firstly the point-wise wave spectrum candidates  $\hat{S}_{ij}(\omega, k)$  are computed by solving (5) through iteration. Secondly, the relative wave direction and the spectrum estimates are found by considering the energy in the candidates.

wave spectrum candidates are compared to get a direction estimate, and the wave spectrum estimate is computed. The imaginary part of the cross spectra  $\mathcal{I}m(R_{z\phi}(\omega))$  is used to distinguish port from starboard sea. The outputs from the estimation algorithm are estimates of the relative wave direction  $\hat{\beta}$  (wave propagation direction  $\hat{\Theta}$  can be calculated), significant wave height  $\hat{H}_s$ , peak period  $\hat{\omega}_p$ , and the wave spectrum  $\hat{S}(\omega)$ .

#### 3.1 Point-wise wave spectrum candidates

Firstly, the frequencies and directions are discretized into  $N_\omega$  and  $N_\beta$  parts, respectively, and the discretized

direction  $k$ , is used to denote directions in the estimation procedure. Since the wave direction is unknown initially, the point-wise wave spectrum candidate needs to be calculated for every direction  $k = \{0, \dots, 180\}$  (one side of the port/starboard symmetric vessel hull), and hence the wave spectrum candidate is dependent on the direction as well as frequency,  $\hat{S}_{ij}(\omega, k)$ . The method does not assume a wave spectrum shape, or parametrize it in any way, and hence the initial wave spectrum estimate and estimate of the response spectrum are set to zero,  $\hat{S}_{ij}(\omega, k) = 0$  and  $\hat{R}_{ij}(\omega, k) = 0$ . For each response pair  $ij = \{zz, \phi\phi, \theta\theta, z\phi, z\theta, \phi\theta\}$  and for each direction  $k = \{0, \dots, 180\}$ , repeat the following steps,

$$\hat{R}_{ij}(\omega, k) = \left| X_i(\omega, k) \overline{X_j(\omega, k)} \right| \hat{S}_{ij}(\omega, k) \quad (5a)$$

$$\tilde{R}_{ij}(\omega, k) = |R_{ij}(\omega)| - \hat{R}_{ij}(\omega, k) \quad (5b)$$

$$\hat{S}_{ij}^+(\omega, k) = \hat{S}_{ij}(\omega, k) + h_{ij}(\omega, k) \tilde{R}_{ij}(\omega, k) \quad (5c)$$

until a threshold is reached

$$\sum_{\omega} \left| \tilde{R}_{ij}(\omega, k) \right| \leq \varepsilon_{ij}, \quad \varepsilon_{ij} > 0. \quad (6)$$

In (5a) a response spectrum estimate  $\hat{R}_{ij}(\omega, k)$  is calculated, in (5b) the response spectrum estimation error  $\tilde{R}_{ij}(\omega, k)$  is computed by making use of the estimated response spectra and the measured response spectra  $R_{ij}(\omega)$ , and in (5c)  $\tilde{R}_{ij}(\omega, k)$  is used to make adjustments to the estimated wave spectrum  $\hat{S}_{ij}(\omega, k)$ , with a gain  $h_{ij} > 0$ .  $h_{ij}$  is discussed in the next section. The next value of the wave spectrum candidate is denoted  $\hat{S}_{ij}^+(\omega, k)$ . The output from (5) are six point-wise wave spectrum candidates per direction, yielding a wave spectrum candidate matrix of dimension  $6 \times N_{\omega} \times N_{\beta}$ ,

$$\bar{S} = \begin{bmatrix} \hat{S}_{zz}(\omega, 0) & \dots & \hat{S}_{zz}(\omega, k) & \dots & \hat{S}_{zz}(\omega, 180) \\ \hat{S}_{\phi\phi}(\omega, 0) & \dots & \hat{S}_{\phi\phi}(\omega, k) & \dots & \hat{S}_{\phi\phi}(\omega, 180) \\ \hat{S}_{\theta\theta}(\omega, 0) & \dots & \hat{S}_{\theta\theta}(\omega, k) & \dots & \hat{S}_{\theta\theta}(\omega, 180) \\ \hat{S}_{z\phi}(\omega, 0) & \dots & \hat{S}_{z\phi}(\omega, k) & \dots & \hat{S}_{z\phi}(\omega, 180) \\ \hat{S}_{z\theta}(\omega, 0) & \dots & \hat{S}_{z\theta}(\omega, k) & \dots & \hat{S}_{z\theta}(\omega, 180) \\ \hat{S}_{\phi\theta}(\omega, 0) & \dots & \hat{S}_{\phi\theta}(\omega, k) & \dots & \hat{S}_{\phi\theta}(\omega, 180) \end{bmatrix}. \quad (7)$$

The iteration (5) is a set of  $6 \times N_{\beta}$  linear equations that are computationally efficient to solve. In this paper we have used  $N_{\beta} = 19$  directions,  $k = \{0, 10, \dots, 180\}$ , and  $N_{\omega} = 35$ . In the following it is explained how to make the selection of the relative wave direction estimate, considering also the interval  $\beta = (-180, 0]$ , and picking out the wave spectrum estimate from the candidates in (7).

### 3.2 Estimation of wave direction and spectrum

The relative wave direction is found by comparing the wave energy for each direction  $k$  in the candidate wave spectrum matrix  $\bar{S}$ . This means that the wave direction estimate is an *energy-averaged* direction. The significant wave height  $H_s$  is a measure of the total energy in a wave system, and is calculated as follows, for each  $ij = \{zz, \phi\phi, \theta\theta, z\phi, z\theta, \phi\theta\}$ :

$$H_{ij}(k) = 4\sqrt{m_{0,ij}}, \quad m_{0,ij} = \int \hat{S}_{ij}(\omega, k) d\omega \quad (8)$$

The result is collected in a matrix with dimensions  $3 \times N_{\beta}$ ,

$$\bar{H}_s = \begin{bmatrix} H_{zz}(0) & \dots & H_{zz}(k) & \dots & H_{zz}(180) \\ H_{\phi\phi}(0) & \dots & H_{\phi\phi}(k) & \dots & H_{\phi\phi}(180) \\ H_{\theta\theta}(0) & \dots & H_{\theta\theta}(k) & \dots & H_{\theta\theta}(180) \\ H_{z\phi}(0) & \dots & H_{z\phi}(k) & \dots & H_{z\phi}(180) \\ H_{z\theta}(0) & \dots & H_{z\theta}(k) & \dots & H_{z\theta}(180) \\ H_{\phi\theta}(0) & \dots & H_{\phi\theta}(k) & \dots & H_{\phi\theta}(180) \end{bmatrix}. \quad (9)$$

For each direction  $k$ , the variance of  $H_{ij}(k)$  is calculated, and the direction candidate is taken as the column of  $H_{ij}(k)$  with the lowest variance, i.e.,

$$\hat{\alpha} := \arg \min_k (\text{var}(H_{ij}(k))), \quad (10)$$

for  $ij = \{zz, \phi\phi, \theta\theta, z\phi, z\theta, \phi\theta\}$ . Notice that  $\hat{\alpha} \in (0, 180]$ , since the iteration is computed for half of the hull. The relative wave direction estimate  $\hat{\beta}$  is found by identifying if the waves are coming from the port or starboard side of the vessel. To do this the imaginary part of the cross spectra  $\mathcal{I}m(R_{z\phi})$  (or  $\mathcal{I}m(R_{\phi z})$ ) are used. The heave response is *symmetric* about the x-axis (body-frame), and the roll response is *anti-symmetric* about the x-axis. The symmetric and anti-symmetric properties of the responses, are reflected in the imaginary part of the heave-roll cross spectra  $\mathcal{I}m(R_{z\phi})$ , which has opposite sign for port and starboard sea. The imaginary part of the cross-spectra are integrated

$$\Gamma_{ij} = \int_{\omega=0}^{\omega_N} \mathcal{I}m(R_{ij}(\omega)) d\omega, \quad (11)$$

where  $\omega_N$  is the highest frequency. If  $\Gamma_{z\phi} < 0$  then the vessel is in starboard sea and  $\hat{\beta} = (-180, 0)$ , and the opposite for port sea, that is,

$$\hat{\beta} \in \begin{cases} [0, 180], & \Gamma_{z\phi} \geq 0 \text{ (port)} \\ (-180, 0), & \Gamma_{z\phi} < 0 \text{ (starboard)}. \end{cases} \quad (12)$$

The wave spectrum estimate is taken as the spectral estimate in heave for the direction  $\hat{\alpha}$ ,

$$\hat{S}(\omega) = \hat{S}_{zz}(\omega, \hat{\alpha}). \quad (13)$$

The reason is that the estimate using the heave response has been found to be the most consistent (Brodtkorb et al., 2018), and for *online* implementation update rate is important as well as accuracy.  $\hat{H}_s$  and  $\hat{\omega}_p$  are calculated as

$$\hat{H}_s := 4\sqrt{m_0}, \quad m_0 := \int_0^{\infty} \hat{S}(\omega) d\omega \quad (14a)$$

$$\hat{T}_p := \frac{2\pi}{\hat{\omega}_p}, \quad \hat{\omega}_p := \arg \max_x \hat{S}(\omega_x). \quad (14b)$$

## 4. STABILITY ANALYSIS

In order to find suitable values for the gains  $h_{ij}$ , we analyze the sea state estimation error dynamics using discrete Lyapunov analysis.

### 4.1 Error dynamics

The wave spectrum estimation error is

$$\tilde{S}_{ij}(\omega, k) := S(\omega) - \hat{S}_{ij}(\omega, k) \quad (15)$$

The estimation error dynamics are derived in the following:

$$\tilde{S}_{ij}^+(\omega, k) = S^+(\omega) - \hat{S}_{ij}^+(\omega, k) \quad (16a)$$

$$= S(\omega) - \hat{S}_{ij}(\omega, k) - h_{ij} \tilde{R}_{ij}(\omega, k) \quad (16b)$$

We have used that the wave spectrum does not change over time, so that  $S^+(\omega) = S(\omega)$ , see (4). By using (5b) inserted (5a),  $\tilde{R}_{ij}$  can be written as:

$$\tilde{R}_{ij}(\omega, k) = \left| X_i(\omega, k) \overline{X_j(\omega, k)} \right| \left( S(\omega) - \hat{S}_{ij}(\omega, k) \right) \quad (17)$$

$$= \left| X_i(\omega, k) \overline{X_j(\omega, k)} \right| \tilde{S}_{ij}(\omega, k) \quad (18)$$

The error dynamics are

$$\tilde{S}_{ij}^+(\omega, k) = \left( 1 - h_{ij} \left| X_i(\omega, k) \overline{X_j(\omega, k)} \right| \right) \tilde{S}_{ij}(\omega, k). \quad (19)$$

This is a linear, unforced, system where the system matrix  $\left( 1 - h_{ij} \left| X_i(\omega, k) \overline{X_j(\omega, k)} \right| \right)$  is independent of time.

#### 4.2 Lyapunov analysis

**Proposition 1:** Given that the iteration gain  $h_{ij}$  is chosen as

$$h_{ij} < \frac{2}{\left| X_i(\omega, k) \overline{X_j(\omega, k)} \right|}, \quad ij = \{zz, \phi\phi, \theta\theta, z\phi, z\theta, \phi\theta\},$$

and assumptions (A1)-(A3) hold, the origin of the wave spectrum estimation error dynamics (19) is discrete-time uniformly asymptotically stable in the large.  $\square$

In order to simplify the notation of the proof, the arguments  $(\omega, k)$  are left out from the equations.

**Proof:** Using results for discrete-time systems from Kalman and Bertram (1960), Theorem 1\*. We propose the Lyapunov function candidate

$$V(\tilde{S}_{ij}) := \frac{1}{2} \tilde{S}_{ij}^2. \quad (20)$$

$V(\tilde{S}_{ij})$  is a continuous function of  $\tilde{S}_{ij}$ , with  $V(0) = 0$ .

- (i)  $0 < \alpha(\|\tilde{S}_{ij}\|) \leq V(\tilde{S}_{ij})$ , with  $\alpha(\|\tilde{S}_{ij}\|) := \frac{1}{4} \|\tilde{S}_{ij}\|^2$ .
- (ii) We need to show that:

$$V(\phi(\tilde{S}_{ij})) - V(\tilde{S}_{ij}) \leq -\gamma(\|\tilde{S}_{ij}\|), \quad (21)$$

with  $\phi(\tilde{S}_{ij})$  denoting the jump map of  $\tilde{S}_{ij}$  (19), and  $\gamma(\cdot)$  being a positive definite function (non-decreasing) with  $\gamma(0) = 0$ . We have that:

$$V(\phi(\tilde{S}_{ij})) - V(\tilde{S}_{ij}) = \frac{1}{2} (\tilde{S}_{ij}^+)^2 - \frac{1}{2} \tilde{S}_{ij}^2 \quad (22a)$$

$$= \frac{1}{2} (1 - h_{ij} |X_i \overline{X_j}|)^2 \tilde{S}_{ij}^2 - \frac{1}{2} \tilde{S}_{ij}^2 \quad (22b)$$

$$= h_{ij} |X_i \overline{X_j}| \left( \frac{1}{2} h_{ij} |X_i \overline{X_j}| - 1 \right) \tilde{S}_{ij}^2 \quad (22c)$$

$$\leq h_{ij} |X_i \overline{X_j}| \left( \frac{1}{2} h_{ij} |X_i \overline{X_j}| - 1 \right) \|\tilde{S}_{ij}\|^2 \quad (22d)$$

$$= -\gamma(\|\tilde{S}_{ij}\|) \quad (22e)$$

- (iii)  $V(\tilde{S}_{ij}) \leq \beta(\|\tilde{S}_{ij}\|)$ ,  $\beta(\tilde{S}_{ij}) = \|\tilde{S}_{ij}\|^2$ .
- (iv) We have that  $\alpha(\|\tilde{S}_{ij}\|) \rightarrow \infty$  when  $\|\tilde{S}_{ij}\| \rightarrow \infty$ .  $\square$

## 5. IMPLEMENTATION ASPECTS

The sea state estimation algorithm is implemented in a Matlab/Simulink simulation model based on the MSS toolbox (Fossen and Perez, 2004), which can simulate DP vessels in changing sea states. The model that has been used is the NTNU owned research vessel (R/V) Gunnerus, with length,  $L_{pp} = 28.9$  meters and beam  $B = 9.6$  meters.

The algorithm uses motion transfer functions calculated for the vessel using ShipX (Sintef Ocean, 2017), and inputs to the algorithm are the heave, roll and pitch motion of R/V Gunnerus. In this section implementation aspects relating to the calculation of response cross-spectra and choice of gains is discussed.

#### 5.1 Computing cross-spectra

The wave parameters change slowly, however, the relative wave direction may change rapidly since the vessel may change heading, and we would like to capture this effect. Cross-spectral estimation is performed on batches of measurement time series in heave, roll and pitch, with an overlap to make sure some data can be re-used, as illustrated in Figure 2. The time it takes before the estimation algorithm has reached *steady state* is

$$T_{tr} = N_{FFT} \frac{1}{F_s} \left( \frac{100 - \mu}{100} \right) N_{avg} \quad (23)$$

where  $N_{FFT}$  is the number of samples used in the spectral calculation,  $F_s$  is the sampling frequency in Hertz,  $\mu$  is the overlap of the dataset in percent, and  $N_{avg}$  is the number of data sets that are averaged for the final result. We would like  $T_{tr}$ , to be as small as possible, while maintaining the accuracy of the estimates.

When a limited number of data points is used, the accuracy of the estimation procedure is affected. Therefore, examining the energy in the wave spectrum candidates is sometimes not sufficient to distinguish head from following sea. Therefore a correction for head/following sea is made in a similar way to port/starboard in (12) by using  $R_{z\theta}(\omega)$ .

$$\hat{\beta} \in \begin{cases} (0, 90), & \Gamma_{z\theta} < 0 \text{ (following)} \\ [90, 180], & \Gamma_{z\theta} > 0 \text{ (head)}. \end{cases} \quad (24)$$

#### 5.2 Choosing gains $h_{ij}$ and tolerances $\varepsilon_{ij}$

From the stability analysis we have that

$$h_{ij} < \frac{2}{\left| X_i(\omega, k) \overline{X_j(\omega, k)} \right|}, \quad ij = \{zz, \phi\phi, \theta\theta, z\phi, z\theta, \phi\theta\}. \quad (25)$$

In order to be conservative we can choose

$$h_{ij} < \frac{2}{\max_{\omega} \left( \max_k \left| X_i(\omega, k) \overline{X_j(\omega, k)} \right| \right)}.$$

For R/V Gunnerus, the largest values of the roll and pitch motion transfer function amplitudes are rather small: 1.1267 and 0.1323, respectively. Therefore an estimate of the largest allowable gain are for some response pairs large:

$$h_{zz} < 1.0282, \quad h_{\phi\phi} < 1.5756, \quad h_{\theta\theta} < 114.2857, \quad (26a)$$

$$h_{z\phi} < 1.7297, \quad h_{z\theta} < 18.1500, \quad h_{\phi\theta} < 58.2625. \quad (26b)$$

These thresholds seem to be valid, as for  $h_{zz} = 1.5$  the simulation is slower, and for  $h_{zz} = 2$  the simulation stops. The findings are similar for the other degrees of freedom. We would like to emphasize that the values in (26) are case specific, depending on the vessel considered and its operating conditions (draught, speed, etc.).

If the tolerance  $\varepsilon_{ij}$  is too large, the iteration is terminated before information is passed from the response spectrum

estimation error to the wave spectrum estimate. If the tolerance is too small, the iteration may not terminate. Therefore, the gain and tolerance should be chosen with a certain regard for the other.

## 6. RESULTS AND DISCUSSION

The simulation results presented in Section 6.1 is of R/V Gunnerus in DP with heading changes of  $-30^\circ$  every 1000 seconds, starting in head sea. The total duration of the simulation is 8000 seconds, and the simulated motion measurements (heave, roll, pitch) are computed using a given (theoretical) wave spectrum together with the actual (wave-to-motion) transfer functions of R/V Gunnerus. The incident wave parameters and tuning of the sea state estimation algorithm are given in Table 1. In Section 6.2 a discussion of the influence of changing the parameters in the estimation procedure is discussed.

Table 1. Summary of the parameters for the simulation case presented in Figure 3.

Waves	
Wave spectrum	JONSWAP
	$H_s = 2$ m, $\omega_p = 0.523$ rad/s, $\gamma = 3.3$
Direction	$\Theta = 180^\circ$ , no spread
Realization	Number of wave components: 300 Number of frequencies: 500
Estimation algorithm	
Spectral estimation	$N_{FFT} = 2048$ , $F_s = 10$ Hz, $N_{avg} = 8$ , $\mu = 75\%$
Gains	$h_{zz} = 1$ , $h_{\phi\phi} = 1$ , $h_{\theta\theta} = 80$ , $h_{z\phi} = 1$ , $h_{z\theta} = 10$ , $h_{\phi\theta} = 30$ ,
Tolerances	$\varepsilon_{ij} = 0.01$ , $ij = \{zz, \phi\phi, \theta\theta, z\phi, z\theta, \phi\theta\}$

### 6.1 Simulation results

In Figure 3, the sea state estimation results for wave conditions and parameters in Table 1 are shown. On the top three plots the time series of the estimates of significant wave height, peak frequency and relative wave direction are given in blue. The three lower plots show the wave spectrum estimate in blue, for three different times: 900, 1900 and 7200 seconds. The incident wave spectrum and the associated parameters are indicated by the dashed red lines. Note that the (stochastic) wave realizations in the simulations may deviate from the (deterministic) generating spectrum given as input.

The estimation algorithm has a transient behavior due to initialization during approximately the first 400 seconds, which corresponds well with  $T_{tr} = 409.6$  seconds (6.67 minutes). The significant wave height oscillates within  $\pm 0.25$  meters, with a small offset from the incident value, peak frequency within  $\pm 0.1$  rad/s, and the heading follows, more or less with a lag of  $T_{tr}$  seconds, with some exceptions. The relative direction estimate deviates a lot around  $T_{tr}$  seconds after many of the heading changes, which is a result of the algorithm analyzing non-stationary data. The value the direction estimate jumps to is always the port or starboard equivalent to the true relative direction, which is not a coincidence. In this sea state the vessel catches up with the waves as it is turning, making the waves in a certain time frame appear to come from the

port or starboard equivalent direction. To avoid jumps in the heading,

- the data set during the transient could be excluded, with the algorithm holding the previous values.
- the relative wave direction estimate could be fixed during the transient, and for  $T_{tr}$  time after.
- logic that contains memory of the direction estimate could prevent the relative wave direction from jumping port/starboard.

### 6.2 Discussion of parameter values

How long  $T_{tr}$  is allowed to be should be dependent on the operation taking place. If the operation keeps one heading for a long period of time, the algorithm can use a long time history of the vessel motion, but if the vessel changes heading frequently,  $T_{tr}$  should be as short as possible. Below is a discussion of how the different parameters in  $T_{tr}$  influences the estimation performance.

- $N_{avg} = \{8, 16\}$  and  $N_{FFT} = \{1024, 2048, 4096\}$ : For lower values,  $\hat{H}_s$  and  $\hat{\omega}_p$  oscillate more, and have higher maxima and lower minima, and  $\hat{\beta}$  jumps more often, and back and forth, after heading changes. Higher values of both  $N_{avg}$  and  $N_{FFT}$  stabilizes the estimates, but increases the transient time, making the direction estimate off for longer periods of time after a heading change.
- $\mu = \{50, 75, 90\}\%$ : Increasing the data overlap may increase the responsiveness of the algorithm for large  $N_{avg}$  and  $N_{FFT}$ . However, with large data overlap, little emphasis is placed on the most recent response data.
- $F_s = \{10, 50, 100\}$ Hz: For 100 Hz the response spectra are broad, and so the wave spectrum estimate is broad as well. So the wave spectrum estimate for 100 Hz is further away from the true wave spectrum than for 50 and 10 Hz, but the wave parameters are still in the correct magnitude ranges. For 10 Hz,  $N_{FFT}$  should be reduced in combination with larger  $\mu$ , so that the transient time is not so large.

## 7. CONCLUSION

The sea state estimation algorithm presented in this paper estimates the onsite sea state well, with limited knowledge of the history of the vessel motion, and with small computational effort. It was shown that an updated estimate can be given every 400 seconds. For further work, the problems with jumps in direction estimate should be solved. It would be interesting to develop a form of auto-tuning both with regards to the gains and tolerances in the algorithm, and with regards to how large  $T_{tr}$ , and allowing for changing batch sizes having in mind the operation status of the vessel.

## REFERENCES

- Brodtkorb, A.H., Nielsen, U.D., and Sørensen, A.J. (2018). Sea state estimation using vessel response in dynamic positioning. *Applied Ocean Research*, 70, 76 – 86. doi: 10.1016/j.apor.2017.09.005.
- Fossen, T.I. (2011). *Handbook of Marine Craft Hydrodynamics and Motion Control*. Wiley.

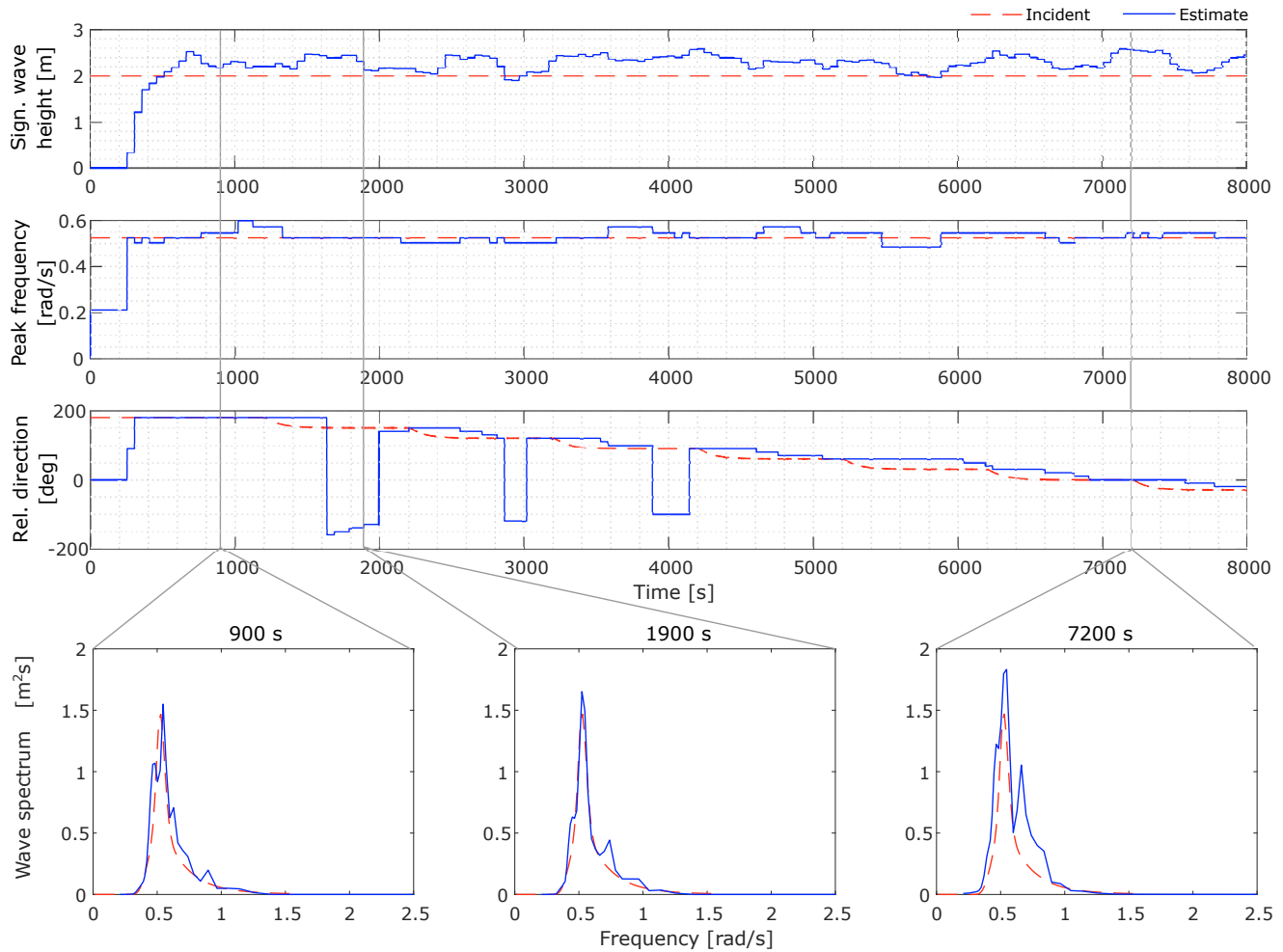


Fig. 3. Sea state estimation results. Above: time series of significant wave height, peak period and wave direction estimates. Below: wave spectra at selected times. Estimates are in blue, and the incident wave parameters are indicated by the red dashed line.

Fossen, T.I. and Perez, T. (2004). Marine systems simulator (MSS). URL <http://www.marinecontrol.org>.

Iseki, T. (2010). Real-time analysis of higher order ship motion spectrum. *ASME. 29th International Conference on Ocean, Offshore and Arctic Engineering*, 2, 399–405. doi:10.1115/OMAE2010-20521.

Kalman, R.E. and Bertram, J.E. (1960). Control system analysis and design via the second method of Lyapunov: II— Discrete-time systems. *ASME. Journal of Basic Eng.*, 82, 394–400. doi:10.1115/1.3662605.

Ludvigsen, M. and Sørensen, A.J. (2016). Towards integrated autonomous underwater operations for ocean mapping and monitoring. *ARC*, 42, 145–157.

Montazeri, N., Nielsen, U.D., and Jensen, J.J. (2016). Estimation of wind sea and swell using shipboard measurements – a refined parametric modelling approach. *Applied Ocean Research*, 54, 73 – 86. doi: 10.1016/j.apor.2015.11.004.

Nielsen, U.D. (2017). A concise account of techniques available for shipboard sea state estimation. *Ocean Engineering*, 129, 352–362. doi: 10.1016/j.oceaneng.2016.11.035.

Nielsen, U.D., Brodtkorb, A.H., and Sørensen, A.J. (2018). A brute-force spectral approach for wave estimation using measured vessel

motions. *Marine Structures*, 60, 101 – 121. doi: <https://doi.org/10.1016/j.marstruc.2018.03.011>.

Pascoal, R. and Guedes Soares, C. (2009). Kalman filtering of vessel motions for ocean wave directional spectrum estimation. *Ocean Engineering*, 36(6-7), 477–488. doi: 10.1016/j.oceaneng.2009.01.013.

Simos, A.N., Sparano, J.V., Tannuri, E.A., and Matos, V.L.F. (2007). Directional wave spectrum estimation based on a vessel 1st order motions: Field results. *Proceedings of the International Offshore and Polar Engineering Conference*, 1938–1944.

Sintef Ocean (2017). *ShipX*. Trondheim, Norway, <http://www.sintef.no/programvare/shipx/>.

Tannuri, E., Sparano, J., Simos, A., and Da Cruz, J. (2003). Estimating directional wave spectrum based on stationary ship motion measurements. *Applied Ocean Research*, 25(5), 243–261. doi: 10.1016/j.apor.2004.01.003.

WAMIT Inc. (2017). *WAMIT- State of the art in wave interaction analysis*. Massachusetts 02467-2504 USA, <http://www.wamit.com>.

Welch, P.D. (1967). The use of fast fourier transform for the estimation of power spectra: A method based on time averaging over short modified periodograms. *IEEE Transactions on Audio and Electroacoustics*, 15, 70–73.